

# A Robust Fusion Method for Motion Artifacts Reduction in Photoplethysmography Signal

Seyedfakhreddin Nabavi, *Member, IEEE*, and Sharmistha Bhadra, *Member, IEEE*

**Abstract**— Robustness of estimating cardiorespiratory parameters from photoplethysmography (PPG) signal is highly dependent on the quality of the signal, which heavily affected by motion artifacts. To increase the estimation accuracy of cardiorespiratory parameters, the present work describes a novel fusion method to efficiently and effectively reduce the motion artifacts from the acquired PPG signal. The proposed fusion technique requires simultaneously acquiring data from a PPG sensor and accelerometer. To filter out the frequencies associated with motion, the method uses stopband filters with a central rejection frequency and bandwidth determined by the output signal of the accelerometer. Under such, the proposed method to remove the motion artifacts does not depend on the quality of the reference signal and has almost no impact on the nature of PPG signals (i.e., amplitude, baseline, and periodicity). The effectiveness of the proposed method in the suppression of in-band and out-of-band frequencies of motion is numerically and experimentally evaluated. It is shown that the filtered PPG signal has sufficient information to estimate different cardiac parameters such as heart-rate (HR), respiration rate (RR) and blood oxygen saturation (SpO<sub>2</sub>). The motion artifacts free PPG signal obtained using our proposed method can estimate HR, RR, and SpO<sub>2</sub> with an accuracy of above 95%. This level of accuracy confirms the usefulness of the proposed fusion method for accuracy improvement of cardiorespiratory parameters monitoring by the filtered PPG signal.

**Index Terms**—Motion artifacts, fusion, heart-rate, respiration rate, blood oxygen saturation, photoplethysmography (PPG)

## I. INTRODUCTION

CARDIORESPIRATORY parameters such as heart-rate (HR), respiration rate (RR) and blood oxygen saturation (SpO<sub>2</sub>), are recognized as important indicators of cardiovascular diseases. HR can be measured by using electrocardiogram (ECG) signals. Such signals can also be used for RR monitoring [1]. The ECG-based monitoring technique is beneficial in terms of accuracy and reliability [2]. However, it requires placing multiple electrodes at different body locations, making this monitoring technique uncomfortable -especially during movement- and impractical particularly for wearable devices. Furthermore, SpO<sub>2</sub>, as a marker of hypoxia and apnea [3], cannot be acquired from the ECG signals.

The research was supported by Natural Sciences and Research Council of Canada, MEDTEQ and industrial partners: iMD Research and Metropole Dentaire Terrebonne.

The authors are with the Department of Electrical and Computer Engineering, McGill University, Montreal, QC H3A-0E9, Canada (corresponding author S. Nabavi: e-mail: [seyed.nabavi@mcgill.ca](mailto:seyed.nabavi@mcgill.ca)).

Photoplethysmography (PPG) has been identified as a potential alternative to ECG signals. In PPG-based sensing, a single or double light source is used at a specific wavelength. The light reflected from or transmitted through the skin indicates blood flow changes and is measured by a photodetector [4]. The PPG signal periodicity variation contains crucial information about HR, RR, and SpO<sub>2</sub>. Thus, a single PPG sensor unit can offer a standalone multisensory platform for comprehensive monitoring of cardiorespiratory signals. In addition, due to the ease of use and low-cost of PPG sensors in comparison to other devices (e.g., ECG), PPGs are widely implanted in advanced wearable devices, such as Fitbit and smartwatches.

In PPG-based monitoring approaches, motion artifacts adversely disturb the PPG output. These artifacts can be caused by hemodynamic effects [5], tissue deformation and mechanical movement of the sensor [6]. Hence, motion artifacts lead to faults and degrade the overall accuracy and validity of cardiorespiratory parameters monitoring with PPG signals [7]. Several approaches have been proposed in the literature to minimize the motion artifacts in PPG signals.

One widely used method to reduce motion artifacts in the PPG signals is independent component analysis (ICA) [8]. In this method, an assumption of the independence between the PPG signals and motion artifacts has to be met [9]. However, the PPG signals with motion artifacts cannot fully satisfy this prerequisite [10]. Therefore, the accuracy level of this method in many real cases is quite low [11]. Another commonly used method for the removal of motion artifacts is adaptive filtering [12]. This method is advantageous for removing in-band frequency of motion, while its effectiveness is highly dependent on the quality of the designed reference signal [13]. This means that the identified improper reference signal will degrade the capability of the filters to remove the motion artifacts. Since a linear correlation between PPG signal and motion signal is necessary for this technique, the adaptive filter performance in the motion artifacts reduction would be relatively poor if the introduced motion is complex and only accelerometer output is considered for constructing the reference signal [14]. Adaptive filtering with synthetic noise generation methods is an iterative process that is computationally expensive [15]. As a result, reducing motion artifacts by the adaptive filters cannot be effectively implemented in wearable and portable systems because the amount of available power in those type of the systems is relatively low. Thus, computationally efficient approaches are highly desirable.

Another motion artifacts reduction method, which was proposed by Reddy *et al.* [16], is using cycle-by-cycle Fourier Series Analysis (CFSA). The efficacy of this method is dependent on correctly determining periods of the PPG signals, while such an objective can be hardly met for the PPG signals, as the quasi-periodic and nonstationary signals. The usefulness of artificial neural network (ANN) for eliminating the motion artifacts in the acquired PPG signals was discussed in [17]. Obviously, this method requires the training data set, and in order to perform real-time and onboard signal processing has to be implemented on the graphics-processing unit (GPU) or highly advanced microcontroller (e.g., Arm Cortex-M).

The quality of sensor output often varies due to the influence of disturbances in the environment, such as motion, temperature. A practical method to deal with these disturbances is fusing signals from multiple sensors. In the past, it has been shown that the sensor fusion technique by using the outputs of different biomedical sensors can increase the overall robustness and accuracy of the measurement [18]. In this context, we propose a novel sensor fusion technique by acquiring data from a PPG sensor and accelerometer to reduce the motion artifacts in the recorded PPG signals. The motion artifacts reduction is performed by filtering out the frequencies of motion through stopband filters. The lower and upper bands of the stopband filters are defined based on the measured accelerometer signal frequencies. The performance of our proposed methodology is not dependent on the quality of a certain reference signal and can reduce the motion artifacts effectively and efficiently.

The contributions of this study can be summarized as follows:

1. We propose a less complex sensor fusion technique, which can be readily implemented on the basic processor platforms, i.e., microcontrollers, for PPG-based wearable and portable systems.
2. The capability of the proposed method in the suppression of motion artifacts is not dependent on the quality of reference signal, hence, the reference signal does not need any preprocessing or conditioning.
3. Our proposed method is able to remove effectively and efficiently both in-band and out-of-band frequencies of motion, while it performed with almost no impact on the nature of PPG signals (i.e., amplitude, baseline, and periodicity).
4. Analysis and measurement show that the filtered PPG signals by our proposed method have sufficient information to accurately estimate multiple cardiorespiratory parameters, i.e., HR, RR, and SpO<sub>2</sub>.

The remaining parts of this manuscript are constructed as follows. Section II describes the working principle of our proposed method to remove motion artifacts. The estimation of cardiorespiratory parameters is briefly discussed in Section III. Numerical and experimental results, as well as discussion, are provided in Section IV. Finally, Section V provides concluding remarks and describes our future work.

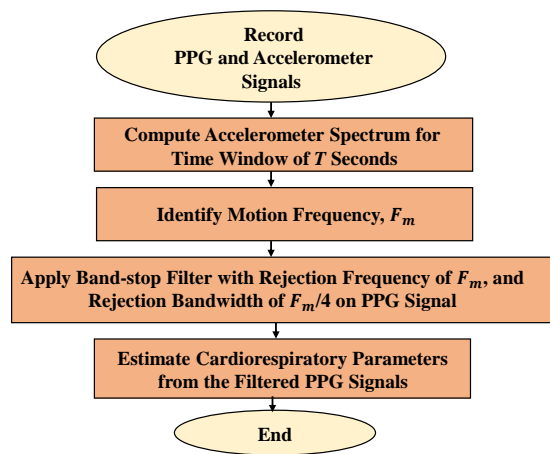


Fig. 1. Working principle of the proposed fusion method for efficient motion artifacts reduction.

## II. METHODOLOGY

The working principle of our proposed motion artifacts reduction method is shown in Fig. 1. According to this figure, in addition to the PPG sensor, an accelerometer has to be deployed to measure the movements of the subject. Therefore, the PPG and accelerometer signals need to be recorded simultaneously. Afterward, a small-time window with  $T$  seconds is sliding on the accelerometer output signal to compute its spectrum. As a result, the frequency of motion is identified for  $T$  seconds. In the next step, a stopband filter, whose central rejection frequency,  $F_m$ , chosen based on the accelerometer spectrum, is applied to the PPG signal captured in the same time window, i.e.,  $T$ . The PPG signal baseline includes information about RR and it is necessary to keep nature of the PPG signals unchanged after performing filtering. Consequently, the width of the stopband filters has to be relatively narrow. In our method, a quarter of the central rejection frequency,  $F_m/4$ , is assumed to be the width of the stopband filter. It is worth mentioning that multiple stopband filters can be also deployed if different frequencies of motion are recognized in the accelerometer spectrum for time window  $T$ .

## III. ESTIMATION OF CARDIORESPIRATORY PARAMETERS

### A. Heart-rate (HR)

One of the widely utilized methods to extract HR from the PPG signals is the analysis of frequency response of the PPG signals, namely, Singular Spectrum Analysis (SSA) [19]. However, in this work, to reduce the complexity of our computation, we estimate HR from analysis of the PPG signal in the time domain to obtain HR beat per minute (bpm). Therefore, by detecting the peak locations in the PPG signals and obtaining the time difference between two consecutive peaks, as shown in equation (1), the average value of HR can be estimated.

$$\text{HR} = \frac{1}{N-1} \sum_{i=1}^N \frac{60}{t_{i+1} - t_i}, \quad N \geq 2 \quad (1)$$

where  $N$  is the total number of the detected peaks in a certain time, and  $t_i$  is the time when the  $i^{\text{th}}$  peak detect.

### B. Respiration rate (RR)

Another beneficial data that can be extracted from the raw PPG signals is RR. In the literature, it is extensively discussed that respiration induces variation in peak-peak amplitude, intensity, and frequency of the PPG signals, respectively [20]. It should be noted that estimation of RR from PPG signal-especially one with the motion artifacts- has a low accuracy. However, it has been shown that RR can be estimated with an acceptable level of accuracy from respiratory-induced peak-peak amplitude variation or respiratory-induced intensity variation in the PPG signals. Consequently, in this study, after removing the motion artifacts from the PPG signal, analysis of the peak-peak amplitude of the PPG signal in the time-domain is utilized for the monitoring of RR. It is worth pointing out that using time-frequency representation methods cascaded with a particle filtering can further improve the accuracy estimation of RR from respiratory-induced peak-peak amplitude variation in PPG signals [21].

### C. Blood oxygen saturation ( $\text{SpO}_2$ )

$\text{SpO}_2$ , as a percentage of oxygenated hemoglobin, is a ratio of oxygenated and deoxygenated hemoglobin concentrations. In pulse oximetry, different absorption of the light source at two individual wavelengths, typically red and infrared, is utilized for estimating  $\text{SpO}_2$ . It is assumed that ripple of the PPG signals (i.e., AC component) is due to pulsatile arterial blood, and its DC level generates from non-pulsatile arterial blood, venous blood, and peripheral tissues [22]. In a dual-wavelength PPG sensor, after normalizing the pulsatile signal with the non-pulsatile signal the ratio of absorbance can be expressed as follows:

$$R = \frac{\text{AC}_{\text{Red}}/\text{DC}_{\text{Red}}}{\text{AC}_{\text{IR}}/\text{DC}_{\text{IR}}}, \quad (2)$$

By using the following quadric equation, which shows the relationship between the ratio of absorbance and  $\text{SpO}_2$ , the level of blood oxygenation can be calculated as:

$$\text{SpO}_2\% = \alpha R^2 + \beta R + \gamma. \quad (3)$$

where  $\alpha$ ,  $\beta$ , and  $\gamma$  are the calibration coefficients and can be obtained empirically through clinical examinations. With reference to the datasheet of PPG sensor [23] and reported results in [24], the values of -45.06, 30.354, and 94.845 were used as the calibration coefficient of  $\alpha$ ,  $\beta$ , and  $\gamma$ , respectively.

## IV. MATERIALS AND METHODS

### A. Design of the stopband filter

The digital filters can be implemented in two different classes, namely, Finite Impulse Response (FIR) and Infinite Impulse Response (IIR) [25]. It has been shown that the FIR filters are always stable and have a constant delay (i.e., linear phase shift) [26]. Due to these desirable and guaranteed features, we confined our study on the FIR filters. The general governing equation for an FIR filter is expressed by:

$$y[n] = b_0x[n] + b_1x[n-1] + b_2x[n-2] + \dots + b_Mx[n-M]. \quad (4)$$

where  $y[n]$  is the output signal,  $x[n]$  is the input signal,  $b$  is the filter coefficient,  $M$  represents the order of the filter, and  $n$  denotes the total number of data points, respectively. By using the  $z$ -transform, which implies that  $x[n-n_0]$  is equal to  $X(z)z^{-n_0}$ , the transfer function of the FIR filter can be obtained as:

$$H(z) = \frac{b_0z^M + b_1z^{M-1} + b_2z^{M-2} + \dots + b_M}{z^M}. \quad (5)$$

According to equation (5), it is clear that the FIR filter includes  $M$  zeros and poles, while all the poles are located at the origin. In order to devise an ideal FIR stopband filter with the capability of the frequency rejection at  $\omega_0$ , a transfer function with zeros located at  $e^{i\omega_0 t}$  and  $e^{-i\omega_0 t}$  (called desired zeros throughout this paper), where  $t$  is the sampling period, is required. In this regard,  $M$  plays an important role in the functionality of the FIR stopband filters.

The impacts of the order of the filter,  $M$ , on the pole-zero pattern and frequency response of the stopband filter are demonstrated in Fig. 2. It is obvious that when  $M$  has a lower order (i.e. the order of 48) the desired zeros are located far away from the unity circle, which causes low attenuation and considerably wide transition widths. In contrast, by increasing the order of  $M$  to 100 the desired zeros become closer to the unity circle. Thus, the filter attenuation besides of its sharpness is enhanced. Further increment in  $M$  (i.e. the order of 148) results in overlying pairs of the desired zeros at the unity circle. Therefore, the filter response in terms of the attenuation and transition widths is further improved when compared to the stopband filter with the order of 100.

Obviously, increasing the order of the FIR stopband filter can enhance its behavior. However, one cannot ignore that the higher value of  $M$  enlarges the filter delay. Moreover, using the stopband filters with considerably high attenuations (i.e., high orders) may deteriorate the general quality of the PPG signal when there are significant overlaps between spectra of the motion artifacts and PPG signal. Consequently, in our proposed motion artifacts reduction technique to effectively deal with in-band motion artifacts and obtain a moderate filter delay as well as an acceptable level of sharpness, the stopband filters with the median order, i.e., 100, were used. In the following, the capability of the stopband filter with the order of 100 will be discussed through the numerical simulations.

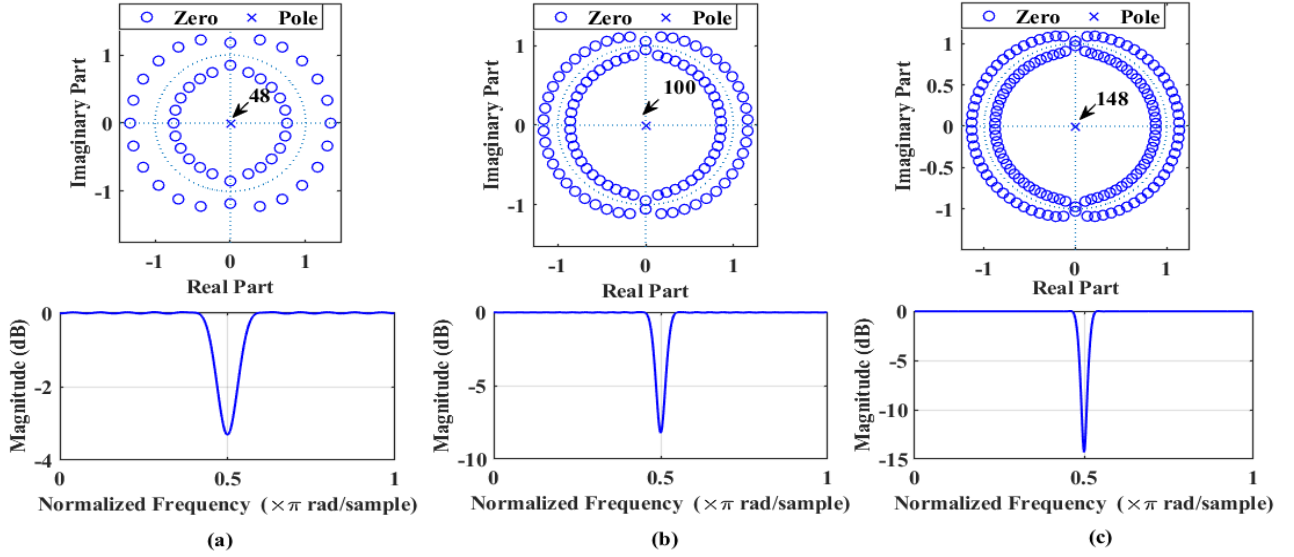


Fig. 2. Pole-zero patterns (top) and frequency spectra (bottom) of the stopband filters with the orders of (a) 48, (b) 100, and (c) 148, respectively.

### B. Numerical simulation

To examine the effectiveness of our proposed technique with the designed stopband filters in the prior subsection, we performed the numerical simulation by using a pure PPG signal, and artificially generated motion artifacts in MATLAB. Indeed, the normal PPG signal is a multi-frequency signal with a frequency band of  $\sim 0.4$ -6 Hz. In Fig. 3 (b1), the frequency response of the PPG signal is demonstrated. It shows that our employed PPG signal comprises three harmonics, i.e.,  $F_1=1.42$ ,  $F_2=3.027$ , and  $F_3=4.49$  Hz, respectively. The computed signal-to-noise ratio (SNR) for this signal is 7.6 dB.

The usefulness of a motion artifacts removal technique is highly dependent on its capability to suppress in-band motion frequency with the minimum effects on the nature of the original signal. Thus, to produce the in-band and out-of-band motion frequencies with sufficient impacts on the morphology of PPG signal, a motion artifact signal at frequencies of  $F_{m1}=1.42$  and  $F_{m2}=6$  Hz, whose amplitude is half of the PPG signal, was generated. The time-domain and frequency-domain of this multi-frequency motion artifacts waveform are demonstrated in Fig. 3 (a2) and (b2), respectively. In Fig. 3 (a3) and (b3), the corrupted PPG signal with artificially generated motion artifacts is presented. This signal has an SNR of 3.95 dB. Apparently, morphology of the PPG signal in the time-domain and frequency-domain is extremely deteriorated. To filter out the frequencies of motion ( $F_{m1}=1.42$  and  $F_{m2}=6$  Hz) two stopband filters with the rejection frequencies corresponding to the motion frequencies were applied.

With reference to the filtering results reported in Fig. 3 (a4), the stopband filters after a relatively small delay, i.e., 0.65 seconds, converged and impacts of the motion artifacts were omitted. Such a small negligible delay will not limit the clinical usages of the proposed method. The frequency spectrum of the filtered signal, as shown in Fig. 3 (b4), confirms that both frequencies of the motion are removed, while the three harmonics of the original PPG signal were preserved. On the

other hand side, the computed SNR for this filtered signal is 5.48 dB, which shows an improvement of 33% in comparison to SNR of the PPG signal with the motion artifacts. Hence, our designed stopband filters can efficiently eliminate the in-band motion frequency, while keep the unique nature of the PPG signal, such as amplitude, spectrum, and periodicity, unchanged.

With reference to the numerical simulation results, it can be concluded that the designed FIR stopband filters with the order of 100 and rejection frequency bandwidth of  $F_m/4$  are able to effectively and efficiently remove the in-band and out-of-band motion artifacts. It is clearly demonstrated that the multi-

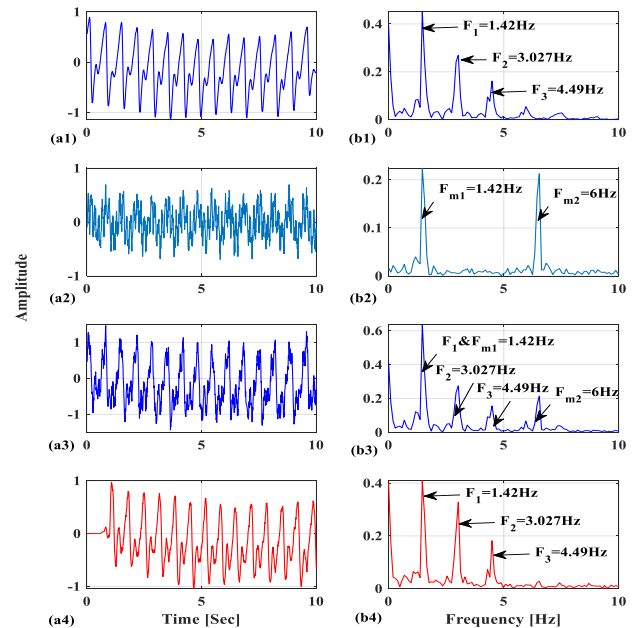


Fig. 3. Numerical simulation for the PPG signal when frequencies of the motion artifacts are in-band of the PPG signal. (a1) Measured PPG signal, (a2) generated motion artifacts waveform, (a3) corrupted PPG signal with the motion artifacts waveform, (a4) filtered signal, and (b1-b4) their corresponding frequency spectra.

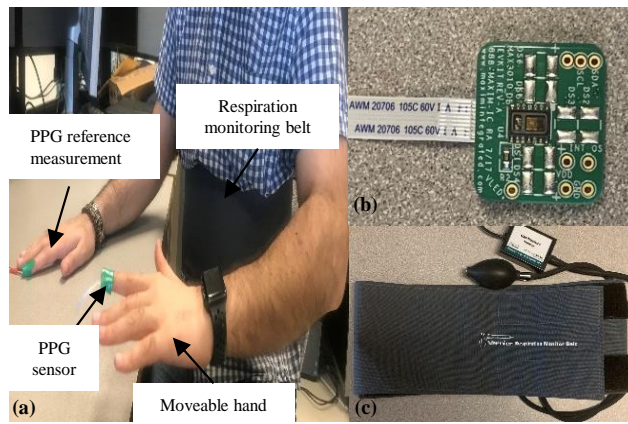


Fig. 4. Photographs of (a) the experimental setup to acquire the affected and unaffected PPG signals and respiratory reference waveform by (b) Max30102 PPG sensor and (c) Vernier respiration monitoring belt, respectively.

frequency motion artifacts within the band of the original signal can be filtered out, while this filtering method has the minimum impacts on nature of the original signal.

### C. Experimental results

In the experimental measurements, as shown in Fig. 4, we used a dual-wavelength, i.e., infrared and red wavelengths, PPG sensor module, which comprises an onboard accelerometer (model Max30102 manufactured by Maxim Integrated). Therefore, the PPG signals and accelerometer output can be recorded simultaneously from this module. The PPG sensor was placed on the left index fingertip. In order to provide an unaffected PPG signal as a reference, another PPG sensor was placed on the right index fingertip of the subject. The conventional respiration monitoring belt interfaced with a gas pressure sensor is considered as a reference measurement for RR.

In Fig. 5 (a) and (b), the impacts of motion on the PPG signals

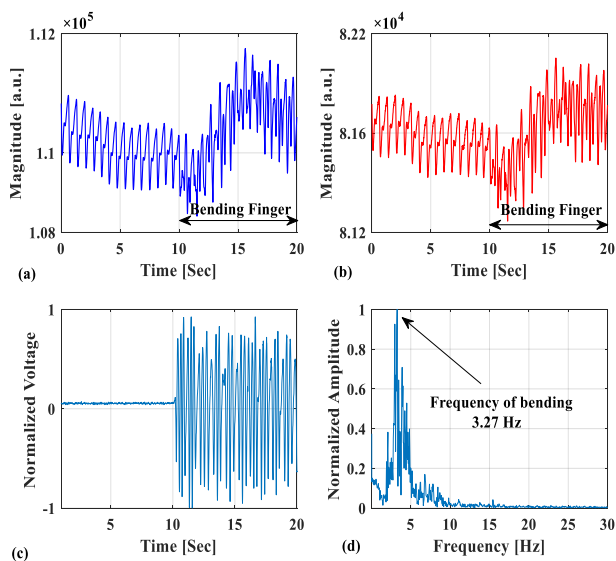


Fig. 5. Impact of motion artifacts on the raw PPG signals at (a) infrared and (b) red wavelengths. (c) The accelerometer output signal and (d) its spectrum.

at both infrared and red wavelengths are illustrated. When bending the left index finger was initiated at instance of 10 seconds a considerable amount of distortion contributed to the acquired PPG signals. The bending of the finger can be accurately monitored by the integrated accelerometer, and spectrum of the accelerometer signal determines the frequency of the finger motion, as shown in Fig. 5 (c) and (d), respectively.

As the first step, superiority of the proposed motion artifacts reduction method in comparison to the conventional adaptive filtering is demonstrated in Fig. 6. As shown in Fig. 6 (b1), the frequency spectrum of the accelerometer signal indicates that the frequencies of the finger bending are about 5 Hz and 10 Hz, while the frequency component at 5 Hz has the maximum impacts on the PPG signal distortion, due to its amplitude. The corrupted part of the PPG signal with this motion artifacts is illustrated in Fig. 6 (a2) and (b2). Obviously, such a corrupted PPG signal cannot be precisely used for extracting all cardiorespiratory parameters, since its morphology got impacted by the motion artifacts in both time-domain and frequency-domain. Therefore, by employing a LMS adaptive filter based on the specifications reported in [27], as the conventional technique for minimizing the motion artifacts, we strived to filter out the frequencies of motion. The result of the adaptive filtering is reported in Fig. 6 (a3) and (b3). We can see that the adaptive filter converged after a few seconds, while the original nature of the PPG signal cannot be fully restored.

The frequency spectrum of the filtered signal by the adaptive filter, i.e., Fig. 6 (b3), shows that the fundamental frequency of

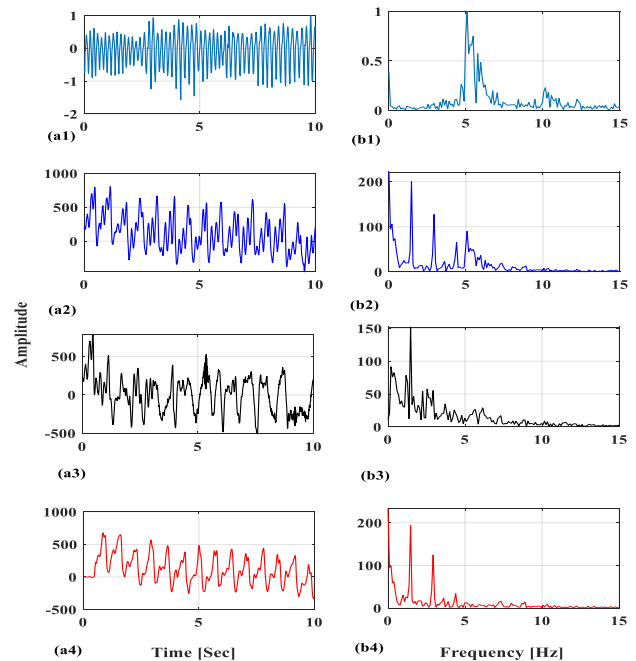


Fig. 6. A comprehensive comparison between the filtered PPG signals at infrared wavelength with the conventional adapting filtering and the proposed motion artifacts removal technique. (a1) Output of the accelerometer, (a2) corrupted PPG signal with the motion artifacts, (a3) filtered PPG signal with the conventional adaptive filtering, (a4) filtered PPG signal by the proposed motion artifacts removal technique, and (b1-b4) their corresponding frequency spectra, respectively.

motion is fully removed and the first harmonic corresponding to HR is preserved. However, other frequency components of the PPG signal considerably deteriorated. Thus, such a filtered signal is mainly beneficial for HR estimation. It is worth reminding that in the literature the adaptive filtering technique was widely used for only HR estimation [28][29][30][27][31].

To the best of our knowledge, so far the PPG signal filtered by the adaptive filtering methods has not been used to simultaneously estimate HR, SpO<sub>2</sub>, and RR. It should be further noted that the preprocessing of the reference signal or optimizing the filter parameters may increase the effectiveness of the adaptive filtering. However, to achieve this objective multiple user-defined parameters have to be wisely chosen.

On the other hand, by implementing the method described in Section II in MATLAB (version 2019a) and the time window,  $T$ , of 20 seconds, the corrupted PPG signal with the frequencies of 5 Hz and 10 Hz was filtered. As shown in Fig. 6 (a4) and (b4), the PPG signal filtered out by our proposed method does not have motion artifacts while almost the nature of PPG signal was preserved. Consequently, this filtered signal has substantial information for estimating different cardiorespiratory parameters. Hence, our proposed method is superior to the conventional adaptive filtering technique.

In order to demonstrate the capability of the proposed methodology for effectively removing even highly complex motion artifacts, the PPG and accelerometer signals were recorded during the subject's left handshaking while keeping the right-hand stable in a sitting position. The frequency spectra of the accelerometer at the x-, y- and z-axis are shown in Fig. 7. It is obvious that each individual accelerometer output can identify  $F_m$  with the maximum discrepancy of  $\pm 0.06$  Hz. Consequently, to minimize the complexity of our proposed methodology, the analysis of only one axis (i.e., x-axis) of the accelerometer was considered.

After determining  $F_m \sim 5$  Hz, the stop-band filter with the central rejection frequency of 5 Hz and rejection bandwidth of 1.25 Hz was applied to both channels of the PPG sensor, whose output signals are affected by the motion discussed in Fig. 7. The capability of our proposed method for removing the motion

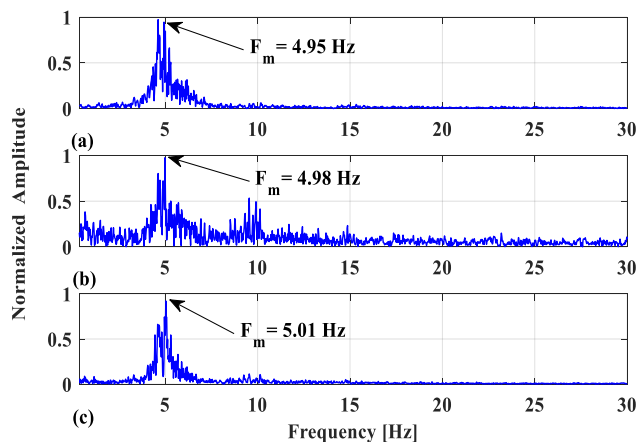


Fig. 7. Frequency spectra of the accelerometer output signals at the (a) x-, (b) y-, and (c) z-axis, respectively.

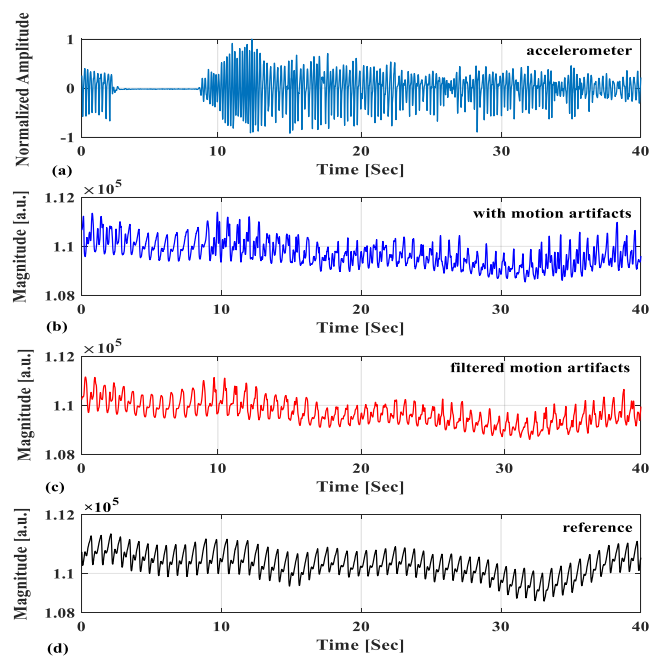


Fig. 8. (a) Motion signal measured by the accelerometer, and the PPG signals (b) with motion artifacts, (c) filtered motion artifacts, and (d) reference signal at infrared wavelength, respectively.

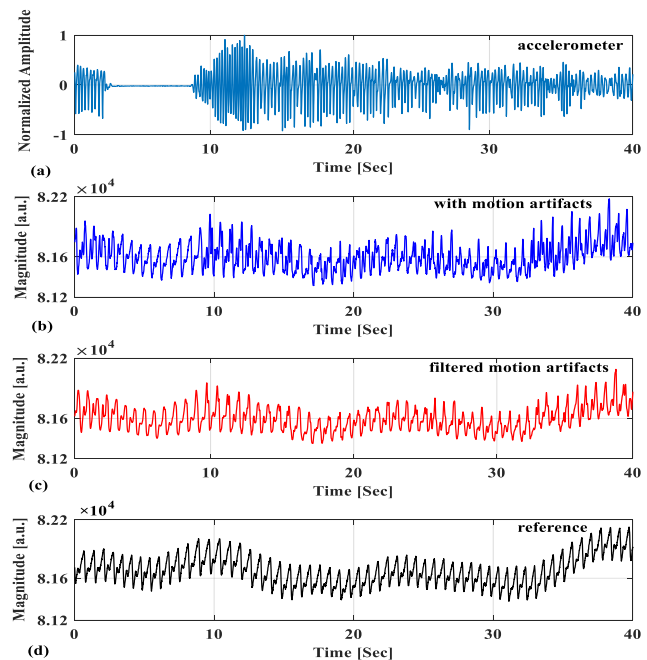


Fig. 9. (a) Motion signal measured by the accelerometer, and the PPG signals (b) with motion artifacts, (c) filtered motion artifacts, and (d) reference signal at red wavelength, respectively.

artifacts at infrared and red wavelengths is shown in Figs. 8 and 9, respectively. It can be seen that our proposed method can remove the motion artifacts effectively at both wavelengths (i.e., infrared and red), while this motion reduction has no impact on nature of the PPG signals, i.e., amplitude and baseline, in addition to the ability of preserving the unaffected region as the original one. As a result, the filtered PPG signals

TABLE I

ESTIMATED VARIANCES OF THE PEAK-PEAK MAGNITUDE AND PEAK-TIME INTERVAL FROM THE PPG SIGNALS WITH MOTION ARTIFACTS, FILTERED MOTION ARTIFACTS, AND REFERENCE MEASUREMENT.

Signal	peak-peak magnitude variance ( $\sigma_{p-p}^2$ )		peak-time interval variance ( $\sigma_{time}^2$ )	
	IR	Red	IR	Red
With motion artifacts	$86.8 \times 10^3$	$9.19 \times 10^3$	$6.1 \times 10^{-3}$	$4.5 \times 10^{-3}$
Filtered motion artifacts	$43.1 \times 10^3$	$3.8 \times 10^3$	$4.7 \times 10^{-3}$	$4.1 \times 10^{-3}$
Reference	$32.5 \times 10^3$	$3.7 \times 10^3$	$4.3 \times 10^{-3}$	$4 \times 10^{-3}$

by the proposed motion artifacts reduction method in this work can be utilized for accurately screening of cardiorespiratory activities.

In order to quantitatively evaluate the behavior of the proposed motion artifacts reduction technique, two metrics, namely, peak-peak magnitude variance ( $\sigma_{p-p}^2$ ) and peak-time interval variance ( $\sigma_{time}^2$ ) are defined. As names of these metrics imply,  $\sigma_{p-p}^2$  determines the variance of peak-peak magnitude of the PPG signal, while  $\sigma_{time}^2$  quantifies variance of the time interval between two consecutive peaks of the PPG signal during a certain time window. In Table I, the computed values of  $\sigma_{p-p}^2$  and  $\sigma_{time}^2$  for the demonstrated PPG signals in Figs. 8 and 9 are listed. As evident from this table, the motion artifacts significantly increase the variation of the PPG signal in terms of the peak-peak magnitude and time interval of the peaks at both wavelengths. Therefore, the maximum amounts of  $\sigma_{p-p}^2$  and  $\sigma_{time}^2$  belong to the PPG signal with the motion artifacts. In contrast, filtering out the motion artifacts by our proposed technique reduced  $\sigma_{p-p}^2$  and  $\sigma_{time}^2$  by 50.23% and 22.9% at infrared wavelength, and by 58.65% and 8.9%, at red wavelength, respectively. A comparison between the variances of the filtered PPG signal and reference measurement deduces that by filtering out the motion artifacts the variances of the filtered signal become closer to the variances of the reference signal, which proves that the filtered PPG signal is in high correlation with reference one, and has the relatively same feature as the reference signal.

To confirm the versatility of the proposed method for increasing monitoring accuracy of cardiorespiratory parameters, the PPG signals were recorded for 40 seconds, while the subject's left hand was randomly shaking to introduce the motion artifacts in the PPG signals. By using the explained approaches in Section III, HR, RR and SpO<sub>2</sub> were estimated from the PPG signals with motion artifacts, PPG signals after filtered motion artifacts and reference ones, respectively, as shown in Figs. 10-12.

In Fig. 10, the estimated HR values from different signals at infrared wavelength are depicted. According to this figure, the estimated HR value from the PPG signal with motion artifacts varied within 79-107 bpm with a mean value of 89 bpm. While the filtered PPG signal illustrated an HR variation between 76 and 100 bpm with a mean value of 88 bpm. On the other side,

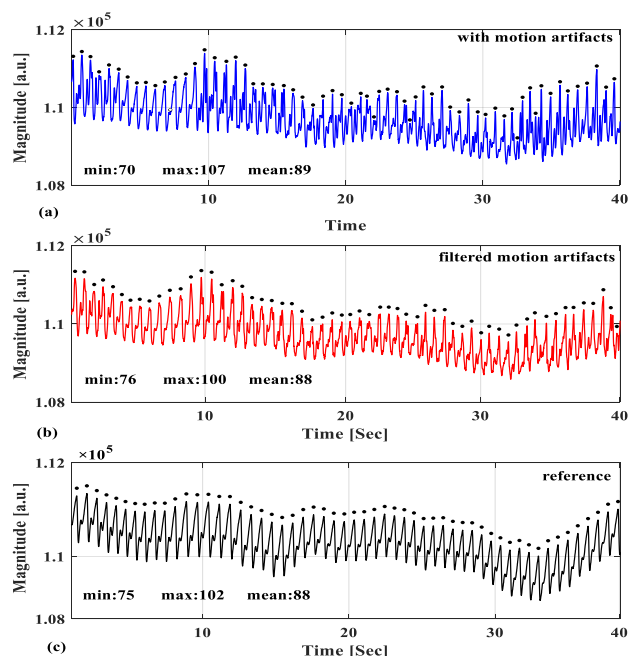


Fig. 10. Estimated HR values with demonstration of the detected peaks as the heart beats from the PPG signals (a) with motion artifacts, (b) filtered motion artifacts, and (c) reference signal, respectively.

the estimated HR value from the reference measurement was in the range of 75-102 bpm with a mean value of 88 bpm. It can be concluded that filtering the PPG signal refines HR values more close to the ones acquired by the reference signal, due to the capability of our proposed method for minimizing the motion artifacts. It should be noted that for identifying the peaks of the PPG signal, a sample point that has the larger value than

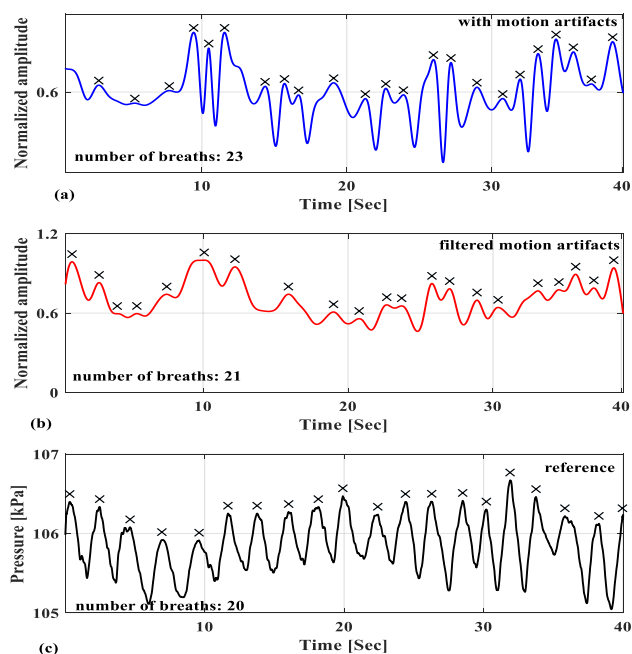


Fig. 11. Estimated respiration waveforms with demonstration of the detected peaks as the breath events from (a) the PPG signal with motion artifacts, (b) the PPG signal after filtering the motion artifacts, and (c) reference signal (respiration monitoring belt), respectively.

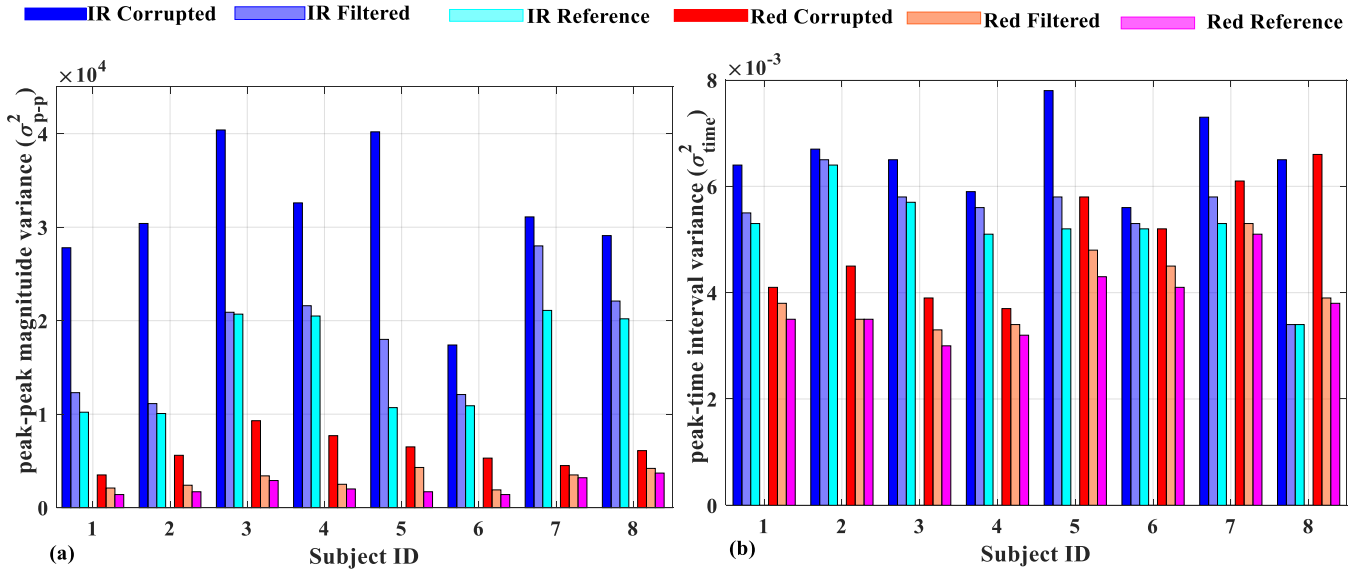


Fig. 13. Quantitative comparison among the computed (a) peak-peak magnitude variance,  $\sigma_{p-p}^2$ , and (b) peak-time interval variance,  $\sigma_{time}^2$ , of the PPG signals with motion artifacts, filtered motion artifacts, and reference measurements for eight subjects.

its two neighboring points within time window of 0.005 seconds (i.e., two times of the sampling rate of 100 Hz) is considered as the local peak.

The impact of the proposed methodology of motion artifacts reduction on monitoring of RR is shown in Fig. 11. The number of observed breathing events in the PPG signal with motion artifacts was 23. After having filtered the signal, the total number of 21 peaks was computed. This provides an accuracy of 95% when compared to the estimated breaths from the reference signal. Thus, removing the motion artifacts from the PPG signal rectifies the respiration waveform, and offers a relatively accurate amount of RR. To detect breathing events in

the respiration waveforms, the data points with the larger values than two neighboring points and threshold of 0.5, in addition to at least 10% descend on either side of the peaks, were identified as the breath events.

The estimated levels of SpO<sub>2</sub> from the PPG signals with motion artifacts, filtered motion artifacts, and reference measurement are shown in Fig. 12. With reference to this figure, the estimated SpO<sub>2</sub> from the PPG signal with motion artifacts is noticeably unreliable, due to its multiple fluctuations, which displays a variation range of 5.9%. However, the measured SpO<sub>2</sub> by the motion artifacts free signals remains robust (i.e., variation range of 0.53%) as is the signal shown in the reference measurement.

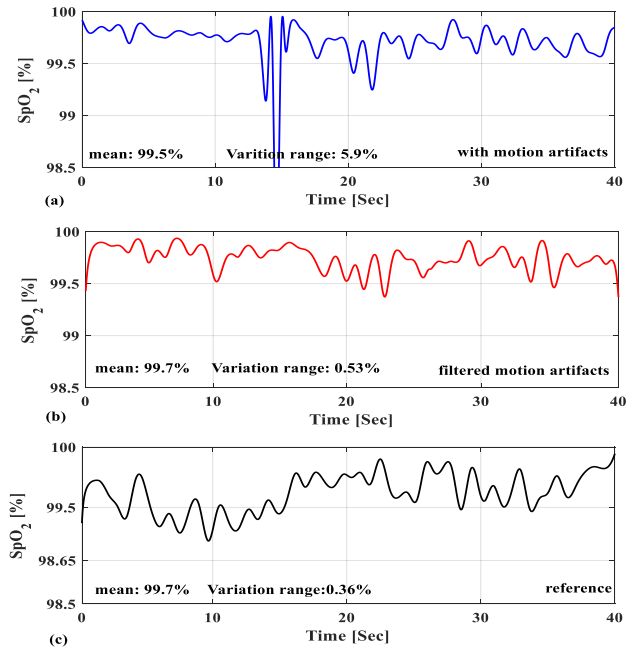


Fig. 12. Estimated SpO<sub>2</sub> levels from the PPG signals (a) with motion artifacts, (b) filtered motion artifacts, and (c) reference signal, respectively.

#### D. Reliability assessment

To this end, it is shown that the motion artifacts reduction methodology described in this study can effectively reduce the impacts of motion, while having almost no impact on the nature of PPG signals. To further confirm that the effectiveness of the proposed motion artifacts reduction technique is not confined to a specific subject, its performance was examined for a group of eight subjects. A similar test, i.e., random left handshaking, was repeated by each subject while keeping the right-hand stable in a sitting position. Thereafter, their HR, RR, and SpO<sub>2</sub> were estimated for the duration of 60 seconds from the PPG signals with motion artifacts, filtered motion artifacts, and reference ones, respectively. In Fig. 13, the computed values of  $\sigma_{p-p}^2$  and  $\sigma_{time}^2$  for the PPG signals with motion artifacts and filtered one, in addition to the reference measurements, for each individual subject at infrared and red wavelengths are depicted. It can be seen at a glance that for all subjects the impact of the motion artifacts has greatly resulted in increasing values of  $\sigma_{p-p}^2$  and  $\sigma_{time}^2$  at both wavelengths when they compared to the variances of reference ones. With reference to this figure, the

TABLE II  
SUMMARY OF THE ESTIMATED HR, RR, AND SpO<sub>2</sub> FROM THE PPG SIGNALS WITH MOTION ARTIFACTS, FILTERED MOTION ARTIFACTS, AND REFERENCE MEASUREMENTS FOR EIGHT SUBJECTS.

Parameters Subject ID	HR [bpm]			RR [breaths/min]			SpO <sub>2</sub> variation range [%]		
	Corrupted	Filtered	Reference	Corrupted	Filtered	Reference	Corrupted	Filtered	Reference
1	79	78	78	19	18	16	3.6	0.3	0.2
2	78	77	76	28	26	25	5.7	0.5	0.6
3	77	76	75	25	23	22	14.2	1	1.1
4	82	81	80	24	22	21	19.8	1.2	0.8
5	81	80	79	22	20	20	7	0.8	1
6	82	80	79	22	20	18	3.2	0.7	0.4
7	76	74	74	20	18	17	3.6	0.5	0.3
8	79	77	76	24	19	20	4.2	0.55	0.4
<b>MAE</b>	<b>2.1</b>	<b>0.8</b>	-	<b>3.1</b>	<b>1.1</b>	-	<b>7.06</b>	<b>0.19</b>	-

maxim signal deterioration occurs for the infrared signal, and the motion artifacts mostly impact on the amplitude of the PPG signal rather than the width of the PPG signal, i.e., peak-time interval. It is worth pointing out that our observation is in good agreement with the literature [32][33].

A holistic comparison among the calculated variances for the filtered and unfiltered PPG signals shows that by filtering the motion artifacts from the corrupted PPG signal the level of variances of  $\sigma_{p-p}^2$  and  $\sigma_{time}^2$  for all the participated subjects, independent on the operational wavelengths of PPG signals, reduced to a certain amount relatively close to the variances of reference measurements. It is also obvious that the variances of the filtered signals never fall less than their corresponding reference variances. Such an observation is repeated for all eight subjects, therefore, it confirms the stable performance of the proposed sensor fusion in preserving the original variability PPG signal content. Consequently, we can conclude that the proposed motion artifacts reduction technique can reliably restore the original features of PPG signal without impacts on its original attributes.

The estimated cardiorespiratory parameters, i.e., HR, RR, and SpO<sub>2</sub> variation range, from the PPG signals with motion artifacts, filtered motion artifacts, and reference measurements for eight subjects are summarized in Table II. According to the computed Mean Absolut Error (MAE) in respect of the reference measurements, as reported at the last row of Table II, our proposed motion artifacts reduction technique can minimize the MAE of HR, RR and SpO<sub>2</sub> variation range from 2.1 bpm, 3.1 breaths/min, and 7.06% to 0.8 bpm, 1.1 breaths/min, and 0.19%, respectively. It is clear that the existence of motion artifacts greatly contributes to variation of SpO<sub>2</sub> ranges, since SpO<sub>2</sub> value is dependent on the quality of both PPG signals at red and infrared wavelengths. It can be also seen that the estimated RR from the PPG signals with motion artifacts is relatively unreliable, because the MAE of 3.1 breaths/min can surely be a sign of respiratory distress. Hence, the proposed method, irrespective of the subject, can substantially improve the accuracy estimation of different cardiorespiratory parameters by eliminating the impacts of the motion artifacts.

By the numerical simulations and experimental measurements, we have shown that the motion artifacts reduction methodology described in this paper effectively removes the motion artifacts with no impact on the nature of PPG signals such as amplitude, baseline, and periodicity. Hence, unlike the conventional approaches discussed in the literature, the rectified outputs of a single PPG sensor by our proposed method can be employed to accurately monitor several cardiorespiratory parameters. In this context, the proposed method does not degrade the original versatility of the PPG signals.

## V. CONCLUSION AND FUTURE WORK

We present a novel sensor fusion technique to substantially reduce the motion artifacts from PPG signals. The functionality of our method does not depend on the quality of the reference signal. The numerical simulations and experimental measurements show the effectiveness of our method in eliminating the motion artifact from the PPG signal while keeping its natural features. The reliability of the proposed technique proves by repeating the experiment for different subjects. Our results indicate that using this motion artifact reduction method provides an accurate estimation of HR, RR, and SpO<sub>2</sub> with an accuracy above 95%. As sensor fusion is becoming popular these days to remove disturbances on sensor measurements, our proposed method will have potential for accurate estimation of cardiorespiratory parameters from the PPG signal.

Looking forward to our future work, we intend to quantify the deterioration level of PPG signal based on the accelerometer outputs information, and accordingly minimize impacts of the motion artifacts. In this regard, we will develop an algorithm to estimate the motion artifacts level and thereafter identify the order(s) of stopband filter(s) based on achieving a clinically acceptable accuracy level for the estimation of cardiorespiratory parameters from PPG signals. To meet such an objective successfully, we will examine a large group of subjects in different positions and motions to determine a general relationship among the motion artifacts level, order(s)

of stopband filter(s), and enhanced accuracy estimation of cardiorespiratory parameters.

## REFERENCES

- [1] M. Schmidt, A. Schumann, J. Müller, K.-J. Bär, and G. Rose, "ECG derived respiration: comparison of time-domain approaches and application to altered breathing patterns of patients with schizophrenia," *Physiol. Meas.*, vol. 38, no. 4, p. 601, 2017.
- [2] V. Krasteva and I. Jekova, "Assessment of ECG frequency and morphology parameters for automatic classification of life-threatening cardiac arrhythmias," *Physiol. Meas.*, vol. 26, no. 5, p. 707, 2005.
- [3] D. Norman *et al.*, "Serum aminotransferase levels are associated with markers of hypoxia in patients with obstructive sleep apnea," *Sleep*, vol. 31, no. 1, pp. 121–126, 2008.
- [4] J. Allen, "Photoplethysmography and its application in clinical physiological measurement," *Physiol. Meas.*, vol. 28, no. 3, p. R1, 2007.
- [5] R. G. Turcott and T. J. Pavlek, "Hemodynamic sensing using subcutaneous photoplethysmography," *Am. J. Physiol. Circ. Physiol.*, vol. 295, no. 6, pp. H2560–H2572, 2008.
- [6] M. T. Petterson, V. L. Begnoche, and J. M. Graybeal, "The effect of motion on pulse oximetry and its clinical significance," *Anesth. Analg.*, vol. 105, no. 6, pp. 78–84, 2007.
- [7] E. Khan, F. Al Hossain, S. Z. Uddin, S. K. Alam, and M. K. Hasan, "A robust heart rate monitoring scheme using photoplethysmographic signals corrupted by intense motion artifacts," *IEEE Trans. Biomed. Eng.*, vol. 63, no. 3, pp. 550–562, 2015.
- [8] M. R. Ram, K. V. Madhav, E. H. Krishna, N. R. Komalla, K. Sivani, and K. A. Reddy, "ICA-based improved DTCWT technique for MA reduction in PPG signals with restored respiratory information," *IEEE Trans. Instrum. Meas.*, vol. 62, no. 10, pp. 2639–2651, 2013.
- [9] B. S. Kim and S. K. Yoo, "Motion artifact reduction in photoplethysmography using independent component analysis," *IEEE Trans. Biomed. Eng.*, vol. 53, no. 3, pp. 566–568, 2006.
- [10] J. Yao and S. Warren, "A short study to assess the potential of independent component analysis for motion artifact separation in wearable pulse oximeter signals," in *Proc. IEEE Engineering in Medicine and Biology*, 2006, pp. 3585–3588.
- [11] Y. Ye, Y. Cheng, W. He, M. Hou, and Z. Zhang, "Combining nonlinear adaptive filtering and signal decomposition for motion artifact removal in wearable photoplethysmography," *IEEE Sens. J.*, vol. 16, no. 19, pp. 7133–7141, 2016.
- [12] M. R. Ram, K. V. Madhav, E. H. Krishna, N. R. Komalla, and K. A. Reddy, "A novel approach for motion artifact reduction in PPG signals based on AS-LMS adaptive filter," *IEEE Trans. Instrum. Meas.*, vol. 61, no. 5, pp. 1445–1457, 2011.
- [13] P. Regalia, *Adaptive IIR filtering in signal processing and control*. Routledge, 2018.
- [14] H. H. Asada, H.-H. Jiang, and P. Gibbs, "Active noise cancellation using MEMS accelerometers for motion-tolerant wearable bio-sensors," in *Proc. IEEE Engineering in Medicine and Biology Society*, 2004, vol. 1, pp. 2157–2160.
- [15] K. A. Reddy and V. J. Kumar, "Motion artifact reduction in photoplethysmographic signals using singular value decomposition," in *Proc. IEEE Instrumentation & Measurement Technology Conference I2MTC*, 2007, pp. 1–4.
- [16] K. A. Reddy, B. George, and V. J. Kumar, "Use of fourier series analysis for motion artifact reduction and data compression of photoplethysmographic signals," *IEEE Trans. Instrum. Meas.*, vol. 58, no. 5, pp. 1706–1711, 2008.
- [17] M. S. Roy, R. Gupta, J. K. Chandra, K. Das Sharma, and A. Talukdar, "Improving photoplethysmographic measurements under motion artifacts using artificial neural network for personal healthcare," *IEEE Trans. Instrum. Meas.*, vol. 67, no. 12, pp. 2820–2829, 2018.
- [18] C. Hoog Antink, F. Schulz, S. Leonhardt, and M. Walter, "Motion artifact quantification and sensor fusion for unobtrusive health monitoring," *Sensors*, vol. 18, no. 1, p. 38, 2018.
- [19] Z. Zhang, Z. Pi, and B. Liu, "TROIKA: A general framework for heart rate monitoring using wrist-type photoplethysmographic signals during intensive physical exercise," *IEEE Trans. Biomed. Eng.*, vol. 62, no. 2, pp. 522–531, 2014.
- [20] M. A. F. Pimentel *et al.*, "Toward a robust estimation of respiratory rate from pulse oximeters," *IEEE Trans. Biomed. Eng.*, vol. 64, no. 8, pp. 1914–1923, 2016.
- [21] M. Pirhonen, M. Peltokangas, and A. Vehkaoja, "Acquiring respiration rate from photoplethysmographic signal by recursive bayesian tracking of intrinsic modes in time-frequency spectra," *Sensors*, vol. 18, no. 6, p. 1693, 2018.
- [22] T. J. Akl, M. A. Wilson, M. N. Ericson, and G. L. Coté, "Quantifying tissue mechanical properties using photoplethysmography," *Biomed. Opt. Express*, vol. 5, no. 7, pp. 2362–2375, 2014.
- [23] "Maxim Integrated." [Online]. Available: <https://www.maximintegrated.com/en/design/reference-design-center/system-board/6300.html>.
- [24] S. K. Longmore, G. Y. Lui, G. Naik, P. P. Breen, B. Jalaludin, and G. D. Gargiulo, "A Comparison of Reflective Photoplethysmography for Detection of Heart Rate, Blood Oxygen Saturation, and Respiration Rate at Various Anatomical Locations," *Sensors*, vol. 19, no. 8, p. 1874, 2019.
- [25] L. R. Rabiner, J. F. Kaiser, O. Herrmann, and M. T. Dolan, "Some comparisons between FIR and IIR digital filters," *Bell Syst. Tech. J.*, vol. 53, no. 2, pp. 305–331, 1974.
- [26] Y. Yamamoto, B. D. O. Anderson, M. Nagahara, and Y. Koyanagi, "Optimizing FIR approximation for discrete-time IIR filters," *IEEE Signal Process. Lett.*, vol. 10, no. 9, pp. 273–276, 2003.
- [27] M. B. Mashhadi, E. Asadi, M. Eskandari, S. Kiani, and F. Marvasti, "Heart rate tracking using wrist-type photoplethysmographic (PPG) signals during physical exercise with simultaneous accelerometry," *IEEE Signal Process. Lett.*, vol. 23, no. 2, pp. 227–231, 2015.
- [28] H. Han and J. Kim, "Artifacts in wearable photoplethysmographs during daily life motions and their reduction with least mean square based active noise cancellation method," *Comput. Biol. Med.*, vol. 42, no. 4, pp. 387–393, 2012.
- [29] L. B. Wood, "Motion artifact reduction for wearable photoplethysmogram sensors using micro accelerometers and Laguerre series adaptive filters," Massachusetts Institute of Technology, 2008.
- [30] M.-Z. Poh, N. C. Swenson, and R. W. Picard, "Motion-tolerant magnetic earring sensor and wireless earpiece for wearable photoplethysmography," *IEEE Trans. Inf. Technol. Biomed.*, vol. 14, no. 3, pp. 786–794, 2010.
- [31] S. H. Kim, D. W. Ryoo, and C. Bae, "Adaptive noise cancellation using accelerometers for the PPG signal from forehead," in *Proc. IEEE Engineering in Medicine and Biology*, 2007, pp. 2564–2567.
- [32] Y. Maeda, M. Sekine, and T. Tamura, "Relationship between measurement site and motion artifacts in wearable reflected photoplethysmography," *J. Med. Syst.*, vol. 35, no. 5, pp. 969–976, 2011.
- [33] J. A. Sukor, S. J. Redmond, and N. H. Lovell, "Signal quality measures for pulse oximetry through waveform morphology analysis," *Physiol. Meas.*, vol. 32, no. 3, p. 369, 2011.



**Seyedfakhreddin (Koorosh) Nabavi** received the B.Sc. degree (Hons.) in biomedical engineering (bioelectric) from the Sahand University of Technology, Tabriz, Iran, in 2013, the M.Sc. degree in electrical and electronic engineering from Ozyegin University, Istanbul, Turkey, in 2015, and the Ph.D. degree from the Memorial University of Newfoundland, St. John's, NL, Canada, in April 2019. He is currently a Postdoctoral Fellow with the Department of Electrical and Computer Engineering, McGill University, Montreal, QC, Canada. His research interests include the design and modeling of MEMS transducers and actuators for industrial and biomedical applications and the design of analog circuits, such as sensor interfaces and power management systems. He has been identified as a Top Reviewer of Applied Physics Letters (APL) in 2018.



**Sharmistha Bhadra** received the B.Sc. degree in computer engineering from the University of New Brunswick, Fredericton, NB, Canada, and the M.Sc. and Ph.D. degrees in electrical engineering from the University of Manitoba, Winnipeg, MB, Canada. From 2015 to 2016, she was an NSERC Postdoctoral Fellow with the University of British Columbia, Vancouver, BC, Canada. She joined McGill University in 2016, where she is currently an Assistant Professor. She has published numerous articles and holds two patents in sensor and wearable area. Her current research interests are in the area of printed and flexible hybrid electronics, microelectromechanical systems, wearables and implants and sensors and actuators.